

IGR J17463-2854, A POSSIBLE SYMBIOTIC BINARY SYSTEM IN THE GALACTIC CENTER REGION

© 2015 D.I. Karasev^{*1}, S.S. Tsygankov², A.A. Lutovinov¹

¹ Space Research Institute, Moscow, Russia

² Tuorla Observatory, University of Turku, Finland

Received 3 March 2015

This paper is devoted to determining the nature of the hard X-ray source IGR J17463-2854 located toward the Galactic bulge. Using data from the INTEGRAL and Chandra X-ray observatories, we show that five point X-ray sources with approximately identical fluxes in the 2–10 keV energy band are detected in the error circle of the object under study. In addition, significant absorption at low energies has been detected in the spectra of all these sources. Based on data from the VVV (VISTA/ESO) infrared Galactic Bulge Survey, we have unambiguously identified three of the five sources, determined the *J*, *H* and *K* magnitudes of the corresponding stars, and obtained upper limits on the fluxes for the remaining two sources. Analysis of the color–magnitude diagrams has shown that one of these objects most likely belongs to a class of rarely encountered objects, symbiotic binary systems (several tens are known with certainty), i.e., low-mass binary systems consisting of a white dwarf and a red giant. Note that all our results were obtained using improved absorption values and an extinction law differing in this direction from the standard one.

Keywords: X-ray sources, symbiotic binary systems, red giants, white dwarfs, interstellar extinction

INTRODUCTION

The X-ray source IGR J17463-2854 was discovered by the INTEGRAL observatory in the survey of the Galactic center region (Bird et al. 2010) and up to now this work has been the only one in which this object was mentioned. The authors determined the coordinates of the source, R.A. = 17^h46^m21^s и Dec. = -28°54′25″, and provided X-ray flux estimates in the 20–40 and 40–100 keV energy bands: ≈ 5 and ≈ 3.1 mCrab, respectively. At the same time, they pointed out that one should not rely on these estimates due to the noticeable “confusion” effect (overlapping of nearby sources), that arises when very crowded sky regions (for example, the Galactic center) are observed by instruments with an insufficient angular resolution. Bird et al. (2010) also point out that the source is transient in nature, but they did not provide its light curves or the time intervals where IGR J17463-2854 was detected in a high state.

Until recently, the lack of the available information and the complexity and crowdedness of the Galactic center region have made it impossible

not only to determine the nature of this source but also to confirm its existence in the first place. In this paper, we have performed for the first time a detailed analysis of the available observational data in different wavelength ranges to determine the emission characteristics and to establish the nature of this object. It is the next one in our series of papers devoted to determining the nature of X-ray sources from the ASCA and INTEGRAL Galactic center surveys (Lutovinov et al. 2015).

INSTRUMENTS AND DATA ANALYSIS

To determine the characteristics of IGR J17463-2854 in hard X rays, we used data from the *ISGRI* detector of the *IBIS* telescope (Ubertini et al. 2003) onboard the INTEGRAL observatory (Winkler et al. 2003) sensitive to photons with energies above 20 keV. The data from this instrument were processed and analyzed in accordance with the methods and algorithms described in Krivonos et al. (2010) and Churazov et al. (2014). It is important to note that in this paper we used the data over all 12 years of INTEGRAL observations, which allowed us to obtain deep maps of the Galactic center region and to investigate the behavior of the source on various

* e-mail: dkarasev@iki.rssi.ru

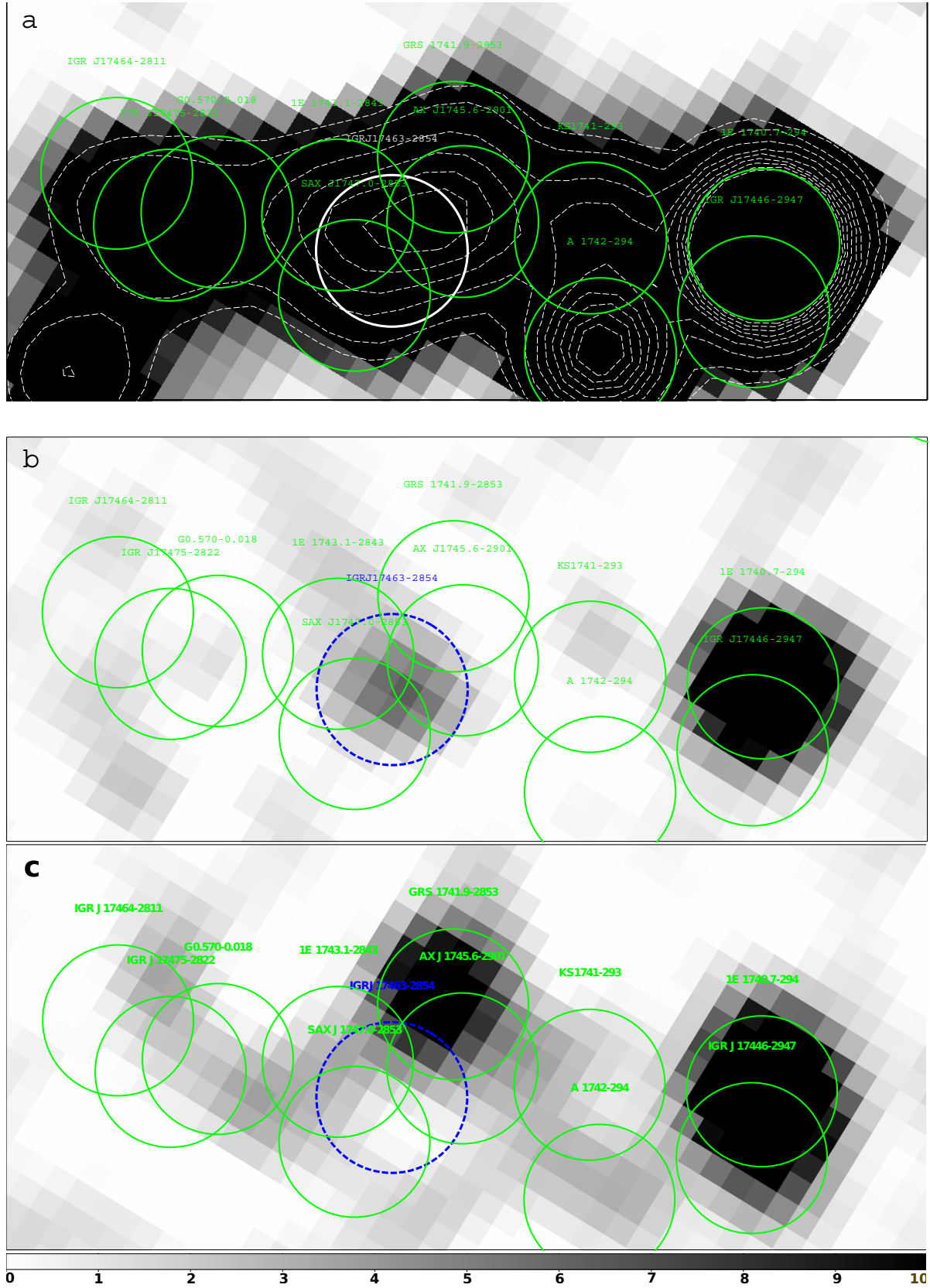


Fig. 1. INTEGRAL images of the sky ($3^\circ \times 1^\circ$) around IGR J17463-2854: (a) the image averaged over the entire time of observations (about 12 years), the outer contour corresponds to a significance level of 10σ , the remaining ones correspond to those from 16.67 to 133.33σ with a step of 16.67σ ; (b) the image averaged over orbits 667, 844, and 1025 in which the object under study was detected with the highest significance; (c) the image obtained for orbit 1201, when IGR J17463-2854 was not detected at a statistically significant level. The image color coding reflects the detection significance and is given in standard deviations. The circle radius is $12'$, corresponding to the angular resolution of the *IBIS* telescope.

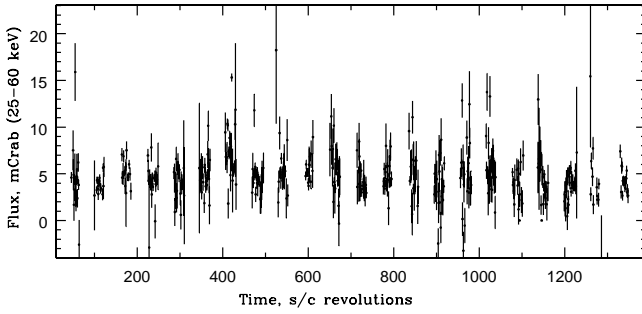


Fig. 2. *IBIS/INTEGRAL* light curve from the error circle of IGR J17463-2854 in the 25–60 keV energy band. The time is specified in units of the *INTEGRAL* orbit (≈ 3 days); the beginning of the first orbit corresponds to the *INTEGRAL* launch date, October 17, 2002 (MJD 52564).

time scales.

To localize the object under study more accurately and to determine its characteristics in the soft X-ray band, we used *Chandra* data, the observations with ObsID 945 (July 7, 2000) and 14 - 897 (August 7, 2013), in which the center of the observatory's field of view was closest to the source localization center in the hard X-ray band. These data were processed using the CIAO-4.7, software package and the CALDB v4.6.5¹. The X-ray spectra of the possible counterparts to IGR J17463-2854 were fitted using the XSPEC v12.7 package.

To identify the object optically and to study its properties in the infrared, we used the VVV/ESO (http://www.eso.org/sci/observing/phase3/data_releases.html), survey, which data for the corresponding sky field were reprocessed using the methods of PSF photometry and the DAOPHOT-II, procedures from the SCISOFT² software package. It was done to obtain more accurate photometric magnitudes of stars in the crowded Galactic center region. To obtain the photometric solutions, we used 2MASS³ as a reference catalog. To check the results of our photometric analysis for correctness, we used data from the UKIDSS/GPS⁴ catalog.

THE HARD X-RAY BAND. INTEGRAL RESULTS

The high density of X-ray sources in the Galactic center region and the insufficiently high angular resolution of the *IBIS/INTEGRAL* telescope (about 12 arcmin) do not allow the total flux to

be separated with confidence between individual objects in the image averaged over the entire time of observations. This fact is illustrated by Fig. 1a, which shows the image of a sky field around the Galactic center in the 25–60 keV energy band obtained over $\simeq 12$ of *INTEGRAL* operation. In particular, it can be seen from this figure that there are four known hard X-ray sources in close proximity to the presumed position of the object under study: – GRS 1741.9-2853, 1E 1743.1-2843, AX J1745.6-2901 and SAX J1747.0-2853.

Nevertheless, owing to the transient nature of all these objects, it turned out to be possible to find the time intervals when IGR J17463-2854 was detected with a higher significance than any of them. As an example, Fig. 1b presents an image of the same sky field as that in Fig. 1a but averaged over three orbits of the observatory (667, 844, and 1025) in which the detection significance of IGR J17463-2854 was at least twice that for other sources. It can be seen that the localization center of the object in this image coincides with the position from Bird et al. (2010) and that its flux during these observations is not affected significantly by neighboring sources and is 10.2 ± 1.1 mCrab in the 25–60 keV energy band ($1 \text{ mCrab} \simeq 9.44 \times 10^{-12} \text{ erg s}^{-1} \text{ cm}^{-2}$ in this band). The light curve obtained from the error circle of IGR J17463-2854 (Fig. 2) shows that this flux is close to the maximum one for the object under study (it should be noted that because of the insufficient angular resolution of the *IBIS* telescope and the influence of neighboring sources, the presented curve is not the light curve of IGR J17463-2854 in the ordinary sense; it more likely reflects the maximum possible fluxes for it at each instant of time).

In the *INTEGRAL* data, there are also periods when IGR J17463-2854 was not detected at a statistically significant level. An example of such a state of the source is presented in Fig. 1c, which shows the same sky field as that in the previous figures but for orbit 1201. It can be clearly seen that another source, GRS 1741.9-2853, was detected at a statistically significant level in this period, while only an upper limit of 2.6 mCrab (3σ , 25–60 keV) can be obtained for the flux from IGR J17463-2854. The noticeable and statistically significant increase in flux observed near the four hundredths orbits is associated with a powerful flare from the transient source SAX J1747.0-2853 located in the immediate vicinity of IGR J17463-2854 and affecting the measured flux from it (Fig. 2). Thus, using all of the available *INTEGRAL* data, we can confirm the existence of a variable hard X-ray

¹<http://cxc.harvard.edu/ciao/>

²<http://www.eso.org/sci/software/scisoft/>

³<http://www.ipac.caltech.edu/2mass/>

⁴<http://surveys.roe.ac.uk/wsa/>

source with coordinates coincident with those from Bird et al. (2010) and a localization accuracy of $\simeq 2.5'$ (Krivonos et al. 2010).

THE SOFT X-RAY BAND. CHANDRA RESULTS

Once we have confirmed that IGR J17463-2854 really exists in hard X-rays and determined its localization accuracy, we can search for and investigate its properties in the soft X-ray energy band. The Chandra X-ray observatory with a high angular resolution is the most suitable instrument for solving this problem. We searched for sources in the Chandra field of view and determined their astrometric positions using the CELLDetect/CIAO procedure. Thus, we detected five point and one extended objects within the INTEGRAL error circle of IGR J17463-2854 at a statistically significant level (Fig. 3). It should be noted that the point objects were known previously and were cataloged in Evans et al. (2010). However, since the sources were closest to the center of the *ACIS* field of view in the observations we used, we managed to localize them with a better accuracy ($\simeq 0.7 - 1''$) than that in the above paper. The corresponding coordinates of the sources are given in Table 1.

Measuring the emission characteristics of the objects detected by Chandra and identifying them with IGR J17463-2854 (searching for the so-called soft X-ray counterpart) were the next step of our studies. Since one of the criteria for the selection of a counterpart among the possible candidates is the hardness of its spectrum, first of all we constructed an image of the error circle of IGR J17463-2854 in two energy bands: 0.5–2 and 2–8 keV (Fig. 3). It can be seen from the figure that all five objects are well detected in the hard channels, with the soft emission from three of them being absent in the 0.5–2 keV energy band, suggesting significant absorption of their emission. The signal from the remaining two sources (nos. 2 and 3) is also registered, but its intensity is considerably lower than that in the 2–8 keV energy band, which also suggests the presence of absorption in the spectra of these sources. In this paper, we used the Chandra data obtained during two pointings spaced more than 10 years apart. Since our analysis revealed no statistically significant changes in the parameters of the spectra for the sources under study, below we summed these observations to improve the statistics.

The spectra of all five sources detected by

Chandra are shown in Fig. 4, while their best-fit parameters are given in Table. 1. We used a simple power law with photoabsorption at low energies to fit the spectra. As has been assumed above, all sources are strongly absorbed and have similar (given the measurement errors) slopes and fluxes. Although the absorption estimates obtained by fitting the X-ray spectra of all sources have significant uncertainties, they show a considerable excess of the hydrogen column density (at solar heavy-element abundances) above the value in standard catalogs for this sky field, $N_H \sim 1.15 \times 10^{22} \text{ cm}^{-2}$ (Kalberla et al. 2005).

It should be noted that we cannot unambiguously assert that intrinsic absorption is present in all sources, because the angular resolution of the neutral hydrogen radio maps (approximately half a degree) is too low to fully take into account all peculiarities of the interstellar medium, especially in such a complex region as the Galactic center. However, we can try to estimate N_H using the infrared extinction data from Gonzalez et al. (2012) obtained with an angular resolution up to $2'$ and the known correlation of the gas and dust distributions in the Galaxy, $A_V = 5.2 \times 10^{-22} N_H$ (Bohlin et al. 1978). The extinction in the V band (A_V) can be estimated by recalculating it from the extinction A_{K_s} in the Ks band (Gonzalez et al. 2012) by assuming that the standard extinction law is valid everywhere (Cardelli et al. 1989; Schlegel et al. 1998). Thus, we can estimate the hydrogen column density to the Galactic center, $N_{H,ir} \simeq 5 \times 10^{22} \text{ cm}^{-2}$, which is comparable, within the error limits, to the derived values for some sources (see Table 1).

However, this approach to estimating the line-of-sight absorption also has shortcomings: there exists a problem that the application of the standard extinction law is limited for the entire sky, especially for the Galactic bulge. In particular, it has been shown in a number of papers that the properties of dust in the Galactic center region can differ from those of local dust; as a result, applying the standard law can overestimate the absorption by up to a factor of 2 (Nishiyama et al. 2009; Revnivtsev et al. 2010; Karasev et al. 2010b). Nevertheless, we may consider the above value as an upper limit on the hydrogen column density for this sky field, and this leads us to conclude that some of the sources have intrinsic absorption. As has been said above, the fluxes from all sources are approximately of the same order of magnitude; nevertheless, source 3 whose flux exceeds the remaining ones approximately by a

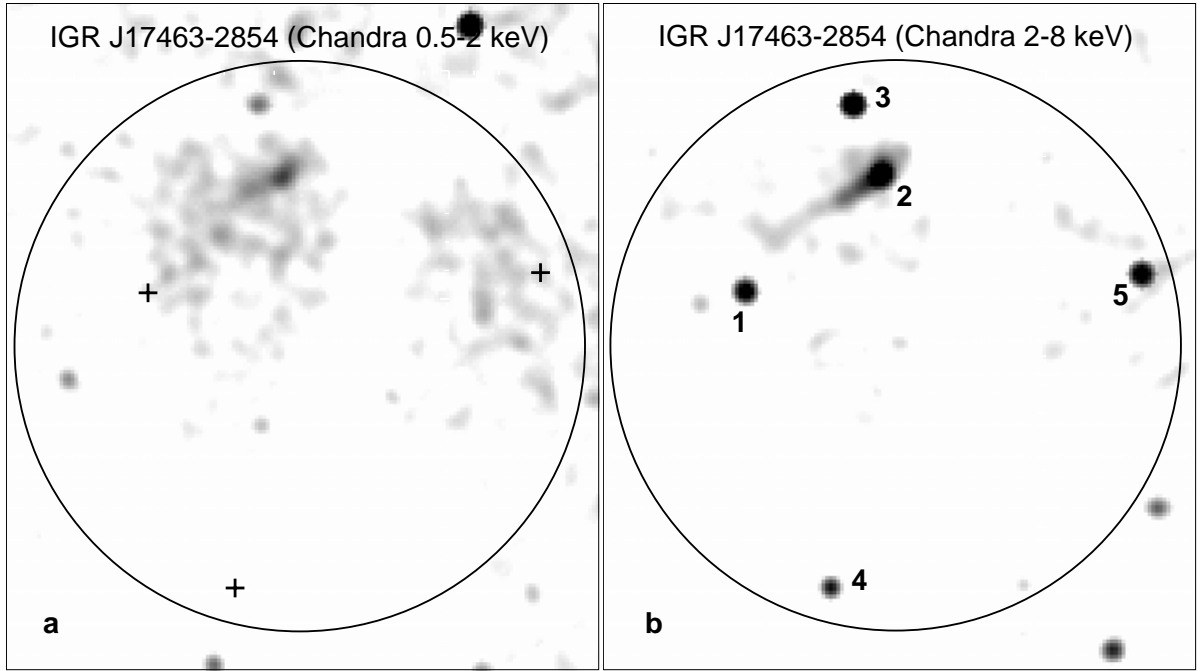


Fig. 3. *ACIS*/Chandra image of the sky around IGR J17463-2854 in two energy bands, 0.5–2 (left) and 2–8 keV (right). The large circle is the INTEGRAL error circle of IGR J17463-2854. The source numbers reflect their distance from the localization center of IGR J17463-2854. The crosses on the left panel indicate the positions of the undetectable sources 1, 4, and 5.

Table 1. Characteristics of the possible soft X-ray counterparts to IGR J17463-2854

#	Name	R.A.(J2000)	Dec (J2000)	Γ	N_H , 10^{22} cm^{-2}	Flux, 2–10 KeV, $10^{-13} \text{ erg/s/cm}^2$	
	Evans et al. (2010)					measured	unabsorbed
1	CXO J174627.0-285356	$17^h 46^m 27^s.022$	$-28^\circ 53' 56''.28$	$0.65^{+0.74}_{-0.64}$	$16.5^{+6.5}_{-5.3}$	$2.15^{+0.74}_{-0.64}$	3.58
2	CXO J174621.6-285257	$17^h 46^m 21^s.578$	$-28^\circ 52' 56''.40$	$1.36^{+0.58}_{-0.50}$	$6.6^{+2.4}_{-1.7}$	$0.79^{+0.13}_{-0.33}$	1.13
3	CXO J174622.7-285218	$17^h 46^m 22^s.724$	$-28^\circ 52' 18''.09$	$0.50^{+0.34}_{-0.30}$	$7.8^{+1.9}_{-1.5}$	$4.73^{+0.70}_{-1.75}$	6.38
4	CXO J174623.5-285632	$17^h 46^m 23^s.599$	$-28^\circ 56' 32''.08$	$0.37^{+0.84}_{-0.69}$	$14.3^{+7.5}_{-5.4}$	$2.06^{+1.43}_{-0.84}$	3.00
5	CXO J174611.3-285346	$17^h 46^m 11^s.218$	$-28^\circ 53' 47''.16$	$0.96^{+0.66}_{-0.59}$	$16.0^{+5.6}_{-4.7}$	$1.89^{+0.25}_{-0.92}$	3.05
	Cloud			$2.12^{+0.27}_{-0.26}$	$6.4^{+0.8}_{-0.7}$	$3.48^{+0.56}_{-1.46}$	5.66

factor of 2–3 can be distinguished among them (see Table 1).

The extended object, the so-called "cloud" located near source 2 and even partially covering it, should be noted separately. The total flux from this cloud in the 2–10 keV energy band is comparable to the flux from source 3 and, together with source 2, exceeds it. Unfortunately, the available data do not allow us to answer the question of whether this cloud and source 2 are associated or are independent objects. Note that the absorption values obtained by fitting the spectra for these objects are virtually equal. Deviations of the measured fluxes from the model spectra are observed in the spectra of sources 1, 4, and 5 in the 6–7 keV energy band (Fig. 4), which may be related to the presence of iron

lines at energies 6.4–7.0 keV in the spectra of these objects. The latter may suggest that they are compact objects, in particular, white dwarfs. Including the emission line at these energies in the model improves the spectrum fitting quality only slightly, with the upper limits (1σ) on the equivalent width of such a line being rather significant, from -0.5 keV for source 5 to 0.6 and 0.84 keV for sources 1 and 4, respectively. Note that such iron line equivalent widths can be observed from white dwarfs in binary systems, for example, from symbiotic stars (see, e.g., Eze 2013).

THE INFRARED BAND. VVV SURVEY RESULTS

To determine the nature of the soft X-ray sources detected by Chandra and, accordingly, the possible

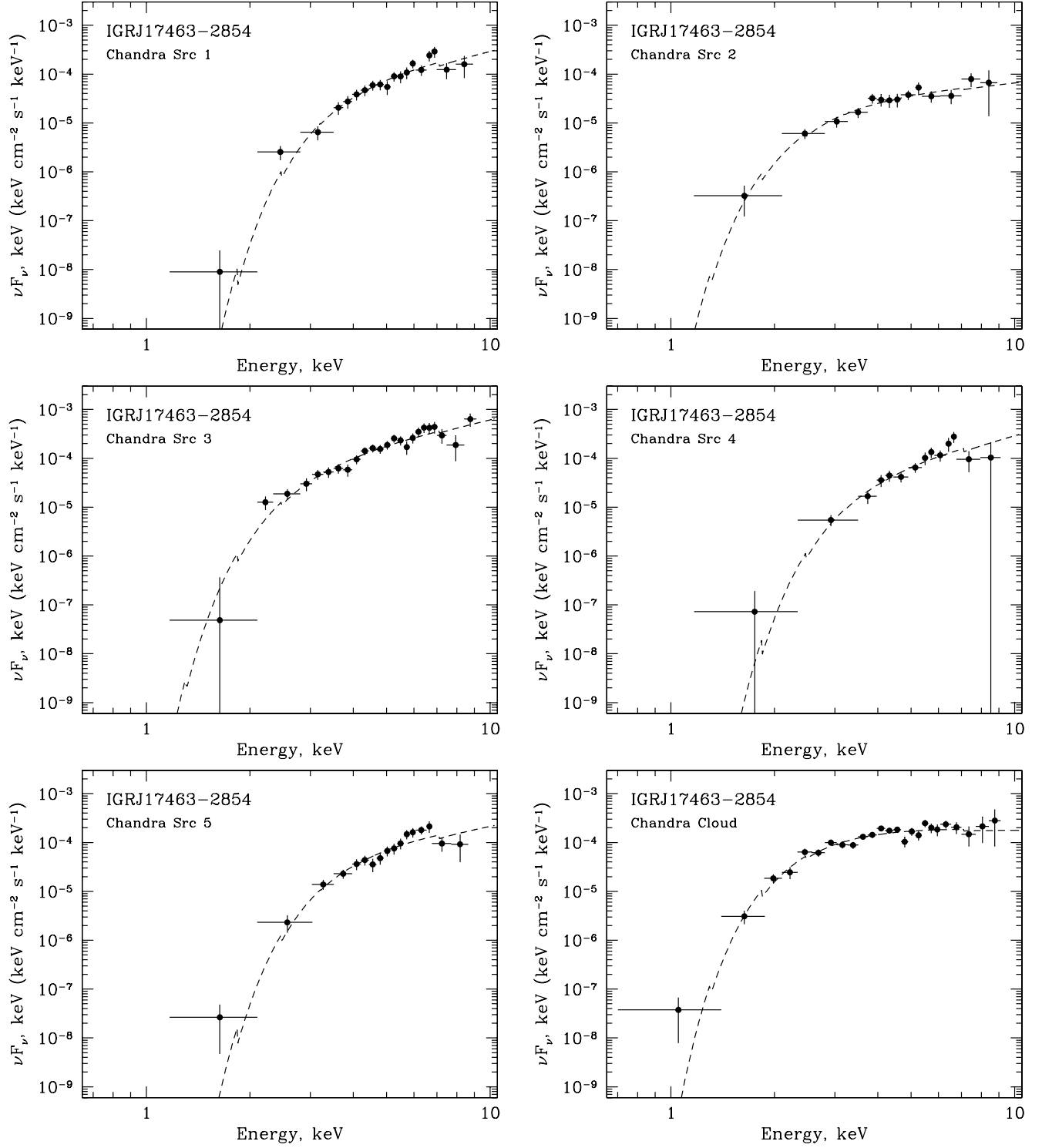


Fig. 4. X-ray spectra of the objects detected by Chandra in the error circle of IGR J17463-2854.

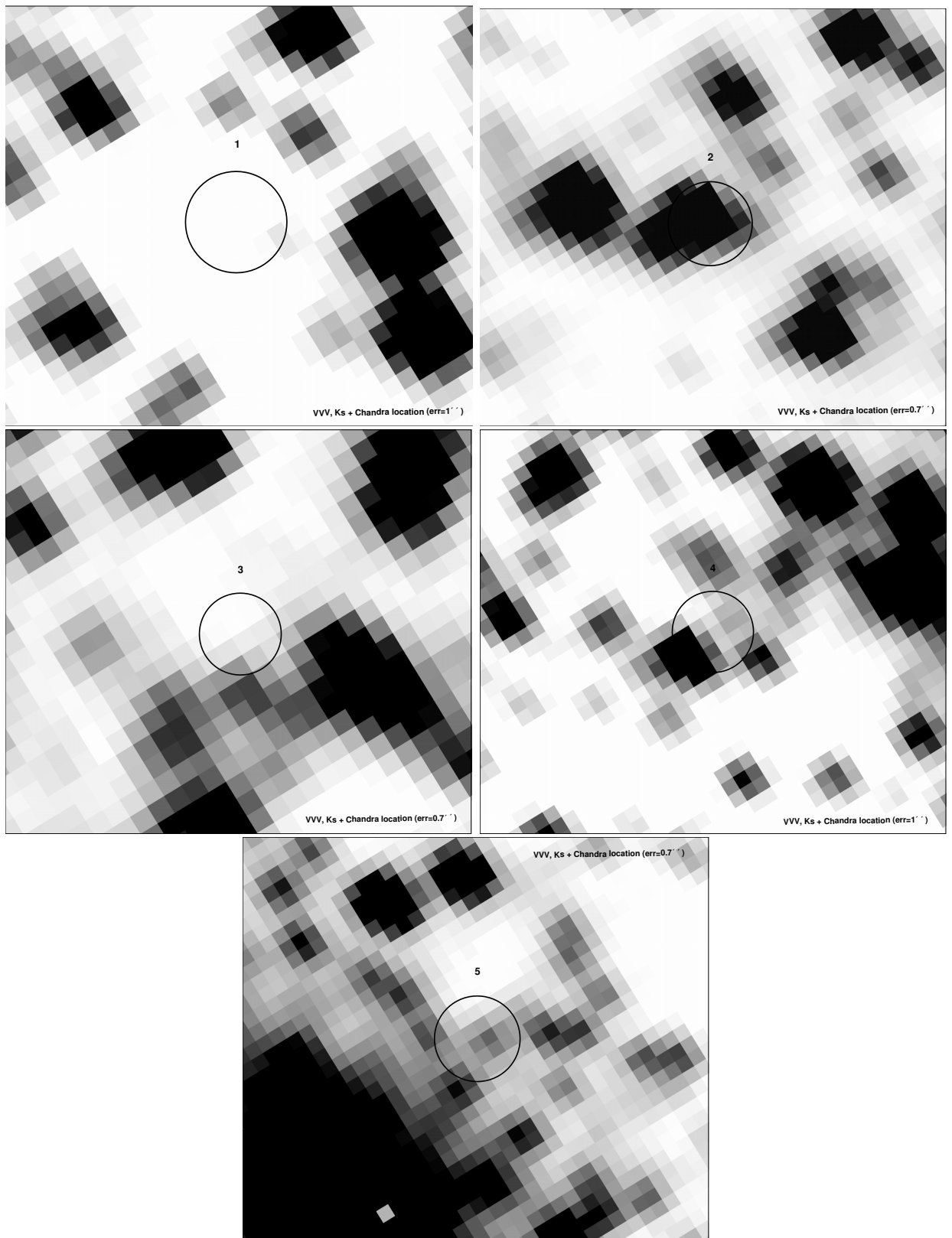


Fig. 5. Image of the sky around the X-ray objects detected by Chandra in the error circle of IGR J17463-2854 in the infrared Ks band based on data from the *VVV* survey. The circles correspond to the Chandra localization accuracy of these objects ($0.7 - 1''$, specified in the images).

Table 2. Infrared magnitudes of the optical counterparts to the sources detected by Chandra

N ^o	m_J	m_H	m_{Ks}
1	> 20.5	> 19.3	> 17.5
2	17.05 ± 0.08	13.54 ± 0.04	11.71 ± 0.02
3	> 20	> 18.7	> 17
4	13.59 ± 0.01	13.03 ± 0.01	12.80 ± 0.02
5	> 19.3	17.06 ± 0.11	15.03 ± 0.06

nature of IGR J17463-2854, we identified them in the infrared energy band based on data from the VVV survey. It can be clearly seen from Fig. 5 that only sources 2, 4, and 5 have a statistically significant identification (their infrared magnitudes are given in Table 2), while sources 1 and 3 do not have such an identification. Since our attempts to identify them using the UKIDSS catalog did not yield any results either, only upper limits on the magnitudes are given for them.

Subsequently, we estimated the classes of the counterparts for sources 2, 4, and 5 based on the approach and the technique from Karasev et al. (2010a) and by taking into account a number of additions related to the peculiarity of the case under consideration. The main idea of this technique is as follows: having the photometric observations of the source located toward the Galactic bulge at least in two filters and knowing the distance and extinction to it (to be more precise, to the red clump giants that are believed to concentrate there), we can identify the classes of the stars that can potentially be counterparts of the X-ray source. It should be noted that variability of the distance to the localization center of the red clump giants (RCGs) along the Galactic bulge is pointed out in a number of papers (see, e.g., Nishiyama et al. 2009; Gonzalez et al. 2012). In the case under consideration, this is not so important, because the objects under study are located toward the Galactic center and the distance to the bulge RCGs in this direction can be assumed to coincide with the distance to the Galactic center. According to the estimates from a number of papers (Paczynski and Stanek 1998; Popowski 2000; Udalski 2003; Revnivtsev et al. 2010; Karasev et al. 2010b), it is determined in the range from 8300 to 8700 pc. For the subsequent analysis, we took the distance to the Galactic center to be $D_{GC} = 8400 \pm 400$ pc.

To determine the extinction to the Galactic center, we investigate the positions of RCGs on the color-magnitude diagram constructed for all stars in some neighborhood ($\sim 1' \times 1'$) of the object under study. A broadening and a local increase in the star density typical of the RCGs are usually

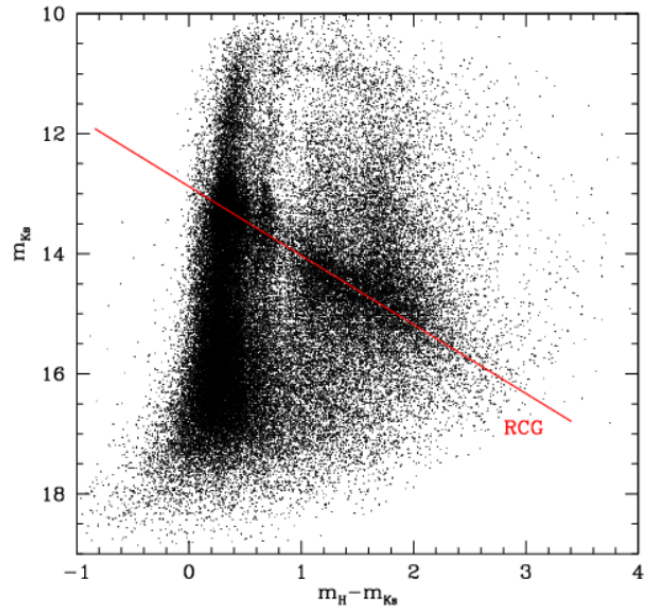


Fig. 6. Cumulative color-magnitude diagram constructed for a $2'$ wide strip symmetric relative to the Galactic plane ($|l| < 1$ deg.) in the vicinity of source 2. The line corresponds to the best fit to the RCG branch by a straight line.

detected on the red giant branch at a statistically significant level. Our analysis showed that for the entire sky field where the sources of interest to us are located, the positions of RCGs on the diagram are virtually invariant and are determined by the following parameters: $m_{Ks,RCG} = 14.60 \pm 0.08$, $m_{H,RCG} - m_{Ks,RCG} = 1.76 \pm 0.15$.

The constructed color-magnitude diagrams give a primary idea of the possible class of the counterpart for some sources (see the left panels in Figs. 7, 8, and 9). In particular, the most probable optical counterpart to source 2 is a fairly bright red giant, because it lies above the clump on the diagram; the infrared counterpart to source 5 is very faint, and all estimates for it have a low significance. However, it also falls, within the error limits, into the region of red giants, but already less bright ones. It can be said about the optical counterpart to source 4 that it is not a red giant.

Returning to the search for and correct determination of the positions of RCGs on the color-magnitude diagram, we will note that the clump is fairly close to the detection limit of the VVV survey for the sky fields under consideration. The latter raises the question as to whether these are actually RCGs or these are just a broadening in the range of faint magnitudes typical for such diagrams. Therefore, we performed an additional study aimed at improving the positions of RCGs

on the color–magnitude diagram in the region of IGR J17463-2854. Since the RCGs in the direction under consideration are at approximately equal distances from the observer, their positions on the color–magnitude diagram depend only on the magnitude and interstellar extinction law (the age and metallicity affect weakly the luminosity of objects from this class; Paczynski and Stanek 1998).

The latter allows us to reveal a local dependence of the observed RCG magnitude on color by investigating the photometric properties of giants in some neighborhood of IGR J17463-2854 and to improve the positions of RCGs on the diagram for the region under study based on the derived dependence. A narrow strip (2' in width) perpendicular to the Galactic plane and covering the range of latitudes from -1 to $+1$ deg. is best suited as such a neighborhood. Owing to the choice of such a region, we can minimize the possible scatter of distances related to the variability of the bulge structure (Nishiyama et al. 2009; Gonzalez et al. 2012).

Figure 6 presents a cumulative color–magnitude diagram for such a strip including the sky field under study. The region of an enhanced star density formed by RCGs is clearly seen on this diagram. The positions of giants can be improved by fitting the derived RCG branch. In addition, the slope of this straight line allows us to determine the extinction law $A_{Ks}/E(H - Ks) = 1.12 \pm 0.11$ toward the bulge for the sky field under study (see also Karasev et al. 2010b), which differs significantly from its standard value of ≈ 1.8 (Cardelli et al. 1989; Schlegel et al. 1998).

Our investigation confirms the validity and correctness of our previous magnitude and color estimates for RCGs toward IGR J17463-2854. Thus, the Ks extinction to the Galactic center in this direction is $A_{Ks,GC} = 1.60 \pm 0.17$, where $A_{Ks,GC} = m_{Ks,RCG} - M_{Ks,RCG} + 5 - 5\log(D_{GC})$, $M_{Ks,RCG} = -1.61 \pm 0.05$ and $M_{Ks,RCG} = -1.61 \pm 0.05$ is the absolute magnitude of RCGs (Alves 2000; Karasev et al. 2010a).

Using this information, we can estimate the class of the counterparts to the sources under study as follows. Considering stars of different spectral types and luminosity classes as a counterpart (by simple exhaustion), we can determine what correction for the extinction ($A_{Ks,test}$) and distance (D_{test}) is required for a star of each of the classes to satisfy the actual observed magnitudes from Table 2.

$A_{Ks,test}$ is determined by comparing the unabsorbed color of a test star $(M_H - M_{Ks})_{test}$ with the color of a real star $((m_H - m_{Ks})_{real})$

for a known extinction law (R), which allows the following quantities in two filters ($A_{H,test}$ and $A_{Ks,test}$) to be related:

$$A_{H,test} - A_{Ks,test} = (m_H - m_{Ks})_{real} - (M_H - M_{Ks})_{test}, \quad (1)$$

$$A_{Ks,test} / (A_{H,test} - A_{Ks,test}) = R. \quad (2)$$

Given the extinction correction, we determine the necessary distance correction:

$$5\log(D_{test}) = m_{Ks,real} - M_{Ks,test} + 5 - A_{Ks,test}. \quad (3)$$

In the next step, we check how these corrections correspond to the previously determined extinction and distance to the Galactic center, our unique reference. If the necessary extinction correction for a star of some class is larger than the extinction to the Galactic center ($A_{Ks,test} > A_{Ks,GC}$), while the distance correction is smaller than the distance to it ($D_{test} < D_{GC}$), then such a star cannot be a counterpart to the source under study in view of a clear mutual contradiction between the corrections. The reverse is also true: if $A_{Ks,test} < A_{Ks,GC}$ and $D_{test} > D_{GC}$, then such a star cannot be a counterpart either. The absolute magnitudes of stars of various classes $M_{Ks,test}$ were taken from Wegner (2007, 2014).

It is necessary to note two important (key) points. First, since we make estimates simultaneously for the extinction and distance, we need to know the observed photometric magnitudes of a star at least in two filters (desirably weakly affected by metallicity) and the extinction law. As has been shown above, the extinction law for RCGs in the direction under consideration differs significantly from the standard one. However, the standard extinction law is valid at close distances (up to several kpc) (Marshall et al. 2006). Since we do not know where and precisely how the extinction law changes, we used the following simplifying assumption: the standard law $R = A_{Ks}/E(H - Ks) = 1.8$ is used closer to the Galactic center ($D < 8400$ pc) and the cumulative nonstandard law $R = A_{Ks}/E(H - Ks) = 1.12$ is used for sources at and behind the Galactic center.

The second key point is how to understand for which classes of stars we should choose the standard law and for which the nonstandard one, i.e., how to understand where a star of some class should have been located before the investigation described above. To answer this question, we used the following simple test. Going sequentially through stars of different classes, we add the distance

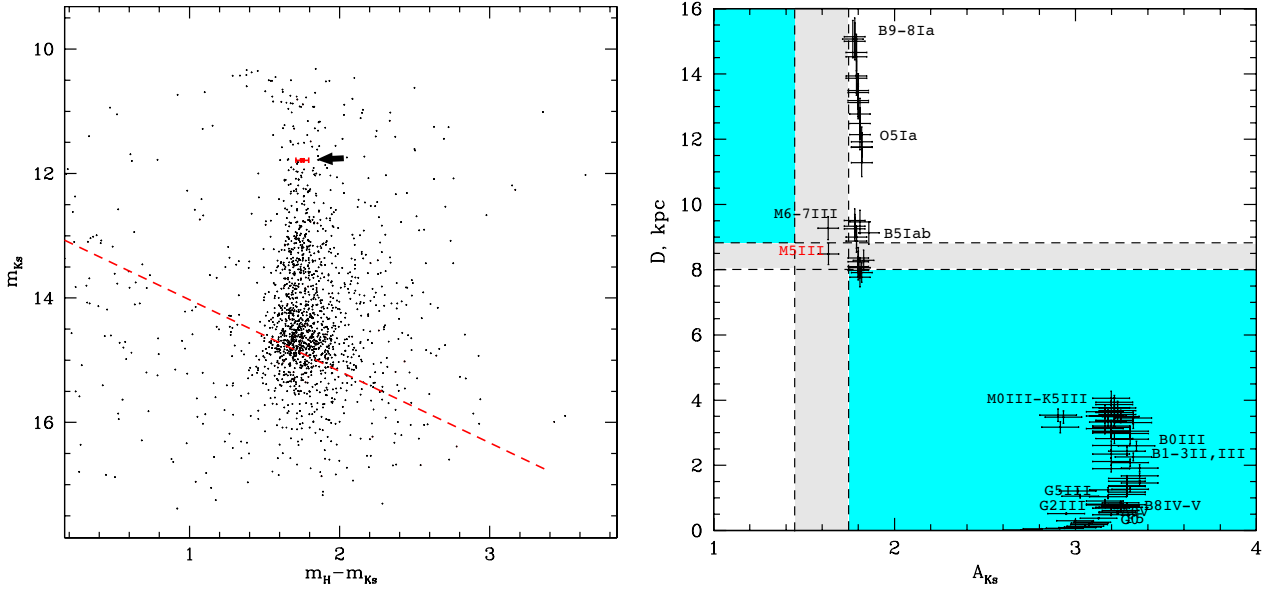


Fig. 7. Left panel: the color-magnitude diagram constructed for a $1'$ neighborhood of source 2; its position is indicated by the square and arrow. The dashed line corresponds to the solid line in Fig. 6. Right panel: the extinction correction-distance diagram showing the distance at which the counterpart to the source of the corresponding class would be located and what extinction it would have. The permitted and "forbidden" classes lie in the white and blue (gray) regions of the diagram, respectively. The light-blue (light-gray) region and the dashed lines reflect the inaccuracy of our knowledge of the distance and extinction to the Galactic center.

and extinction corrections corresponding to the Galactic center to their absolute magnitudes and determine what "apparent" Ks magnitude would be obtained for each tested star, i.e., $m_{Ks, \text{test}, GC} = M_{Ks, \text{test}} + 5 \log(D_{GC}) - 5 + A_{Ks, GC}$. Then, we compare this magnitude with the actually observed Ks of the counterpart of the source (Ks ($m_{Ks, \text{real}}$ from Table 2)). If $m_{Ks, \text{test}, GC} < m_{Ks, \text{real}}$, then the corresponding corrections for the Galactic center are not enough to sufficiently attenuate the star of the chosen class. It turns out that such a star could be a counterpart to the source only if it were farther from the Galactic center. The reverse is also true if $m_{Ks, \text{test}, GC} < m_{Ks, \text{real}, \text{real}}$. Note that the photometric data only in one filter are sufficient for such qualitative estimates of the distance to the star; for the same reason, a change in the extinction law does not affect these estimates.

Having determined the boundaries of applicability of a particular extinction law and applying the technique described above, we can estimate what classes of stars the optical counterparts to sources 2, 4, and 5 most likely are. The results are presented in the form of distance correction-extinction correction diagrams on which the regions of forbidden and permitted combinations are marked by the blue (gray) and white colors, respectively (Figs. 7, 8, and 9, right panels). Note that the "jump" of points on the

diagrams is explained by the application of different extinction laws for stars of different classes.

It follows from these diagrams that the optical star in the system with source 2 is most likely an M5III red giant, although brighter M6-7III stars can also be counterparts to the object because of the errors in determining the distance to the Galactic center and the corresponding extinction. The optical counterpart to source 5 may also belong to the class of red giants (approximately G5III), although stars of other spectral types brighter than B6 cannot be ruled out either, within the error limits (Fig. 9). In comparison with source 2, the color-magnitude diagram gives no unambiguous indication that it is a red giant of the bulge. We cannot say anything certain about the class of the optical counterpart to source 4 from the presented diagram (Fig. 8). Thus, among the five point X-ray sources detected by Chandra in the error circle of IGR J17463-2854, at least one is a possible candidate for a symbiotic binary system. Note that the described tests and methods are valid under the assumption of a fairly uniform growth of the cumulative extinction with distance in the absence of dust cocoons around the sources.

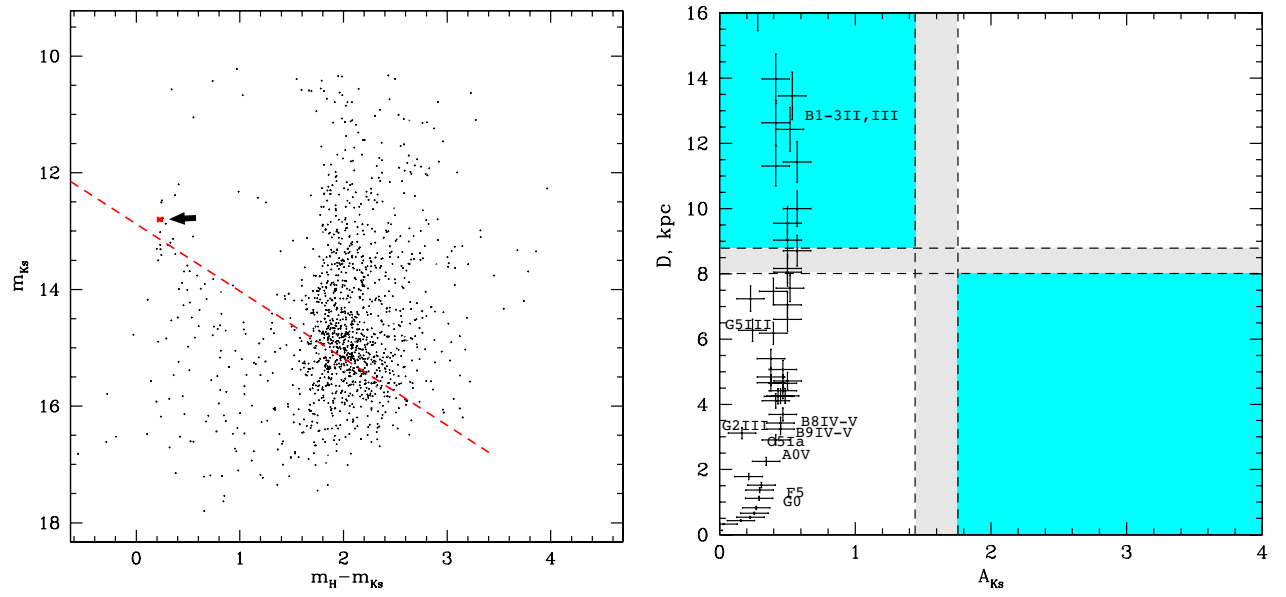


Fig. 8. Same as Fig. 7 for source 4.

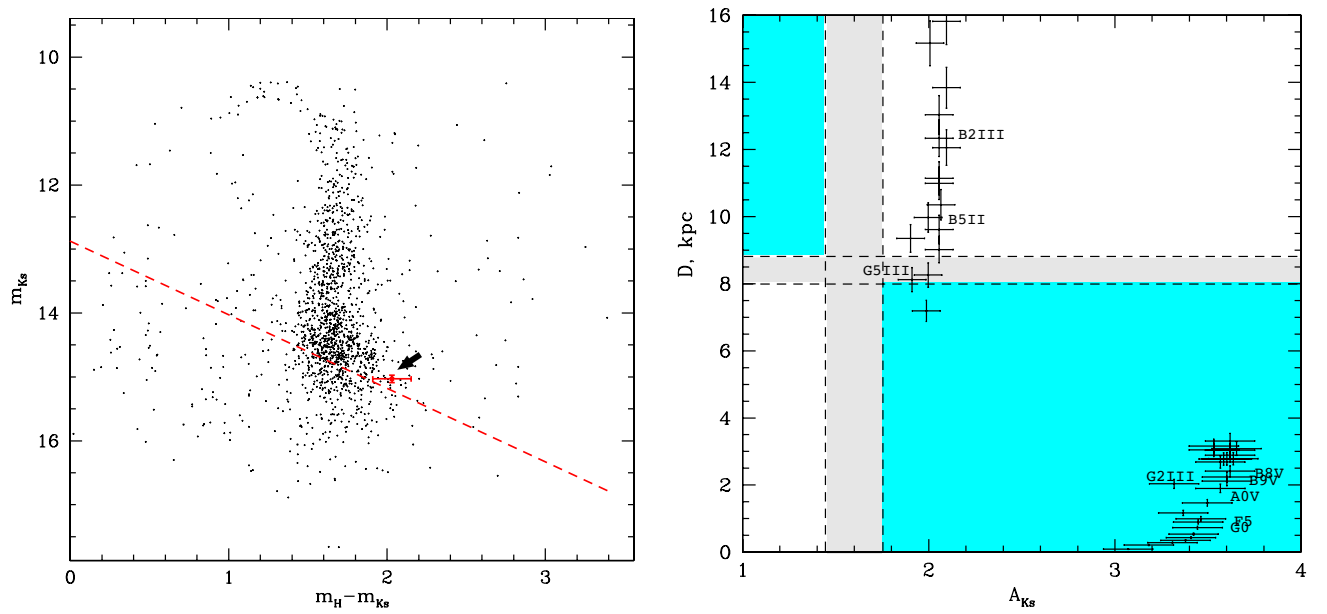


Fig. 9. Same as Fig. 7 for source 5.

CONCLUSIONS

In this paper, we investigated in detail the properties of the poorly studied hard X-ray source IGR J17463-2854. Improving the error circle of this object allowed us to identify it in other energy bands. In particular, according to the Chandra data, five point and one extended objects of comparable intensity are detected at a statistically significant level in the error circle of IGR J17463-2854.

The total flux registered from all these objects in the 2–10 keV energy band is $\simeq 1.5 \times 10^{-12}$ erg s $^{-1}$ cm $^{-2}$. If this flux is rescaled to the 25–60 keV energy band under the assumption of broadband spectra typical of symbiotic stars (Kennea et al. 2009; Eze 2013), neutron stars (Filippova et al. 2005), or active galactic nuclei projected onto the Galactic plane (see, e.g., Sazonov et al. 2004), then the expected flux in this band will be considerably lower than that measured by INTEGRAL. Thus, the hard X-ray flux of $\simeq 10$ mCrab from IGR J17463-2854 cannot be explained by a simple superposition of the persistent fluxes from the objects detected by Chandra. The observed transient behavior of IGR J17463-2854 is most likely related to the variability of the emission from one of the soft X-ray sources. Their variability cannot be revealed on time scales of hundreds and thousands of seconds based on the Chandra data, because the sources are too faint to construct a statistically significant light curve. The observations spaced almost 10 years apart did not reveal any significant changes in the fluxes either.

Nevertheless, based on the results of our studies, we showed that at least one of the objects detected by Chandra in the error circle of the hard X-ray source IGR J17463-2854 is probably a symbiotic system, which are characterized by noticeable flux variability (Yungelson et al. 1995; Kennea et al. 2009; Eze 2013). The relativistic object in it is most likely a white dwarf with a luminosity $L_X \simeq 8.9 \times 10^{32}$ erg s $^{-1}$, while the normal star is an M5–M7III red giant located at the distance of the Galactic center. We cannot say anything unequivocal about the nature of the remaining soft X-ray sources, but their X-ray spectra suggest that they can also be white dwarfs.

In conclusion, note that we also tried out the technique of searching for symbiotic systems in the Galactic bulge based on the results from Karasev et al. (2010a) and improved data on the absorption and extinction law for the Galactic center region (Karasev et al., in preparation).

ACKNOWLEDGMENTS

We thank M.G. Revnivtsev, A.N. Semena, and A.A. Voevodkin for the discussion of our results and useful remarks. We are also grateful to E.M. Churazov, who developed the IBIS/INTEGRAL data analysis methods and provided the software. This work was financially supported by the Russian Science Foundation (project no. 14-22-00271).

REFERENCES

1. D.R. Alves, *Astrophys. J.* **539**, 732 (2000).
2. A.J. Bird, A. Bazzano, and L. Bassani, *Astrophys. J. Suppl. Ser.* **186**, 1 (2010).
3. R.C. Bohlin, B.D. Savage, and J.F. Drake, *Astrophys. J.* **224**, 132 (1978).
4. J. Cardelli, G. Clayton, and J. Mathis, *Astrophys. J.* **345**, 245 (1989).
5. E. Churazov, R. Sunyaev, J. Isern, J. Knodlseder, P. Jean, F. Lebrun, N. Chugai, and S. Grebenev, *Nature* **512**, 406 (2014).
6. I.N. Evans, F.A. Primini, K.J. Glotfelty, C.S. Anderson, N.R. Bonaventura, J.C. Chen, J.E. Davis, and S.M. Doe, *Astrophys. J. Suppl. Ser.* **189**, 37 (2010).
7. R. Eze, *MNRAS* **437**, 857 (2013).
8. E. Filippova, S. Tsygankov, A. Lutovinov, and R. Sunyaev, *Astron. Lett.* **31**, 729 (2005).
9. O.A. Gonzalez, M. Rejkuba, M. Zoccali, E. Valenti, D. Minniti, M. Schultheis, R. Tobar, and B. Chen., *Astron. Astrophys.* **552**, 9 (2012).
10. P. Kalberla, W. Burton, D. Hartmann, E. Arnal, E. Bajaja, R. Morras and W. Poppel, *Astron. Astrophys.* **440**, 775 (2005).
11. D. Karasev, A. Lutovinov, and R. Burenin, *MNRAS* **409**, L69 (2010a).
12. D.I. Karasev, M.G. Revnivtsev, A.A. Lutovinov, R.A. Burenin, *Astron. Lett.* **36**, 788 (2010).
13. J. Kennea, K. Mukai, J. Sokoloski, G. Luna, J. Tueller, C. Markwardt and D. Burrows, *Astrophys. J.* **701**, 1992 (2009).
14. R. Krivonos, M. Revnivtsev, S. Tsygankov, S. Sazonov, A. Vikhlinin, M. Pavlinsky, E. Churazov, and R. Sunyaev, *Astron. Astrophys.* **519**, A107 (2010).
15. A. A. Lutovinov, M. G. Revnivtsev, D. I. Karasev, V. V. Shimanskii, R. A. Burenin, I. F. Bikmaev, V. S. Vorobyov, C. S. Tsygankov, and M. N. Pavlinsky, *Astron. Lett.* **41**, 179 (2015).
16. D. Marshall, A. Robin, C. Reyle, M. Schultheis, and S. Picaud, *Astron. Astrophys.* **453**, 635 (2006).
17. S. Nishiyama, M. Tamura, H. Hatano, D. Kato, T. Tanabe, K. Sugitani, and T. Nagata, *Astrophys. J.* **696**, 1407 (2009).

18. B. Paczynski and K. Stanek, *Astron. Astrophys.* **494**, 219 (1998).
19. P. Popowski, *Astrophys. J.* **528**, 9 (2000).
20. M. Revnivitsev, M. van den Berg, R. Burenin, J. Grindlay, D. Karasev, and W. Forman, *Astron. Astrophys.* **515**, 49 (2010).
21. S. Sazonov, M. Revnivitsev, A. Lutovinov, R. Sunyaev, and S. Grebenev, *Astron. Astrophys.* **421**, L21 (2004).
22. D.J. Schlegel, D.P. Finkbeiner, and M. Davis, *Astrophys. J.* **500**, 525 (1998).
23. P. Ubertini, F. Lebrun, G. Di Cocco, A. Bazzano, A.J. Bird, K. Broenstad, A. Goldwurm, G. La Rosa, et al., *Astron. Astrophys.* **411**, L131 (2003).
24. A. Udalski, *Astrophys. J.* **590**, 284 (2003).
25. W. Wegner, *MNRAS* **374**, 1549 (2007).
26. W. Wegner, *Acta Astronomica* **64**, 261 (2014).
27. C. Winkler, T.J.-L. Courvoisier, G. Di Cocco, N. Gehrels, A. Gimenez, S. Grebenev, W. Hermsen, J.M. Mas-Hesse, F. Lebrun, et al., *Astron. Astrophys.* **411**, L1 (2003).
28. L. Yungelson, M. Livio, A. Tutukov, and S.J. Kenyon, *Astrophys. J.* **447**, 656 (1995).